Single-file diffusion in periodic energy landscapes: The role of hydrodynamic interactions

E. C. Euán-Díaz,[1,2] V. R. Misko,[2] F. M. Peeters,[2] S. Herrera-Velarde,[1] and R. Castañeda-Priego[1,*]

[1]*Division of Sciences and Engineering, University of Guanajuato, Loma del Bosque 103, Lomas del Campestre, 37150 León, Guanajuato, Mexico*

[2]*Department of Physics, University of Antwerpen, Groenenborgerlaan 171, B-2020 Antwerpen, Belgium*

(Received 4 July 2012; published 18 September 2012)

We report on the dynamical properties of interacting colloids confined to one dimension and subjected to external periodic energy landscapes. We particularly focus on the influence of hydrodynamic interactions on the mean-square displacement. Using Brownian dynamics simulations, we study colloidal systems with two types of repulsive interparticle interactions, namely, Yukawa and superparamagnetic potentials. We find that in the homogeneous case, hydrodynamic interactions lead to an enhancement of the particle mobility and the mean-square displacement at long times scales as t^{α}, with $\alpha = \frac{1}{2} + \epsilon$ and ϵ being a small correction. This correction, however, becomes much more important in the presence of an external field, which breaks the homogeneity of the particle distribution along the line and, therefore, promotes a richer dynamical scenario due to the hydrodynamical coupling among particles. We provide here the complete dynamical scenario in terms of the external potential parameters: amplitude and commensurability.

DOI: 10.1103/PhysRevE.86.031123 PACS number(s): 05.40.−a, 47.57.eb, 66.10.cg

I. INTRODUCTION

Colloidal suspensions are made of mesoscopic objects, i.e., colloids, that, even in the absence of any kind of external perturbation, exhibit interesting static and dynamical properties [1]. Furthermore, when the suspension is confined, it shows new features that are not found in the bulk. For instance, in highly restricted geometries, such as quasi-one-dimensional (q1D) and one-dimensional (1D) systems, the long-time mean-square displacement (MSD) follows a subdiffusive non-Fickian behavior, i.e., $W(t) \propto t^{\alpha}$, with $\alpha < 1$ [2–17].

Single-file diffusion (SFD) is the diffusion of particles in q1D geometries where the particles exhibit random-walk movements in channels so narrow that no mutual passage is possible [18]. Rigorous theoretical results for SFD have been derived in detail for the simple case of hard rods [19–22]. It was predicted that the $W(t)$, for times much longer than the direct interaction time τ, i.e., the time that a particle needs to move a significant fraction of the mean particle distance, is given by the relation [23,24]

$$\lim_{t \gg \tau} W(t) = F\sqrt{t}, \tag{1}$$

where F is the so-called SFD mobility factor. Recently, Kollmann [25] reported a theoretical study on the long-time behavior of SFD that is valid for atomic and colloidal systems as long as the interaction is the same and of finite range. For overdamped systems, i.e., colloidal suspensions, Kollmann also showed that the mobility factor can be expressed as [25]

$$F^q = \frac{S(q)}{\rho}\sqrt{\frac{D_c(q)}{\pi}}\bigg|_{q \ll 2\pi/\sigma}, \tag{2}$$

where ρ is the number particle density, σ is the particle diameter, and q, $S(q)$, and $D_c(q)$ are the magnitude of the wave vector, the static structure factor, and the short-time *collective*-diffusion coefficient, respectively, in q space [1].

According to Eq. (2), the long-time character of SFD is thus determined by the short-time *collective* dynamics at long wavelengths; $q \to 0$. In this limit, $S(q) \to S(0)$, where $S(0)$ of monodisperse systems corresponds to the normalized isothermal compressibility [1], which can be measured using either experiments [4] or computer simulations [16]. Furthermore, $D_c(q)$ can be rewritten as $D_c(q) = D_0 H(q)/S(q)$ [1], with D_0 and $H(q)$ the free-particle diffusion coefficient and the hydrodynamic factor, respectively. Using previous expressions in Eq. (2), it now reads

$$F^q = \frac{1}{\rho}\sqrt{\frac{D_0 S(q) H(q)}{\pi}}\bigg|_{q \to 0}. \tag{3}$$

Equations (1) and (3) draw a remarkably simple picture of 1D diffusion at long times: the self-diffusion process, determined by the width of the probability density, is proportional to $t^{1/2}$ and the proportionality constant is determined by the short-time individual particle dynamics, which is a function of the interparticle interactions and density through $S(q)$ and the hydrodynamic coupling given by $H(q)$. If one assumes that hydrodynamic interactions (HIs) can be neglected, i.e., $H(q) = 1$, one finds that the mobility factor reduces to $F^q = \frac{1}{\rho}\sqrt{\frac{D_0 S(0)}{\pi}}$. Lin *et al.* showed that this expression accurately reproduces the mobility factor of hard rods, F^{HR} [4]. Additionally, using hybrid molecular dynamics and the stochastic rotations dynamics computer simulation method, Sané *et al.* corroborated the $\sqrt{t}$ dependence of the MSD of hard rods and found that the particle mobility factor, with the explicit inclusion of HIs, is given by F^{HR} [26].

Recent experiments on charged macroscopic particles (millimetric steel balls) confined in circular channels [27] and a linear channel of finite length [28] exhibited particle diffusion slower than the $t^{1/2}$ behavior. Delfau *et al.* [28] experimentally identified three dynamical regimes, which have recently been studied theoretically [29,30], and found that the particle response to thermal fluctuations strongly depends either on the particle position in the channel or on the local

*ramoncp@fisica.ugto.mx

potential it experiences. The slower diffusion found in the previous experiments can be explained in terms of the lack of an overdamped dynamics in a system composed of steel particles [31].

During the last decade, the influence of interparticle interactions on the SFD of 1D colloidal suspensions has been discussed extensively using experiments, simulations, and theory [2–9,11,13–17,26–42]. However, as far as we know, the effects of HIs on the SFD have seldom been studied [26]. Furthermore, to the best of our knowledge, numerical simulations for high densities or large potential strengths are not available for the case in which HIs are explicitly included. Thus, a natural question that arises is whether the SFD of colloidal systems with different interaction ranges is affected by HIs. This question has been experimentally addressed using 2D colloidal systems composed of superparamagnetic colloidal particles on the air-water interface and exposed to external magnetic fields [43,44]. Authors reported experimental [43] and computer simulation [44] evidence for an enhancement, due to the HIs, of the self-diffusion function, $D_s(t)$, of colloids at intermediate and long times.

Moreover, the action that both external fields and HIs exert on colloidal particles results in interesting hydrodynamic behaviors [45–48]. For example, the motion of a colloidal particle in a strong optical trap reveals that at short time scales resonances in the Brownian motion exist, in contrast to overdamped systems [45]. Besides, the influence of external fields in 1D colloidal systems has been studied [14,15,37,49] without taking into account HIs or in dilute samples [50], where HIs can be simply ignored. In addition, we have to point out that the coupling of external fields with HIs gives rise to a rich dynamical scenario that has not been studied in detail yet.

Thus, the main goal of this work is to understand the effects of HIs on the SFD of repulsively interacting colloidal particles subjected to spatially periodic energy landscapes. We provide the full dynamical description in terms of the external potential parameters, namely, strength and commensurability. We particularly demonstrate that the MSD at long times undergoes subdiffusive behavior of the form $W(t) = Ft^{\alpha}$, with $\alpha = \frac{1}{2} + \epsilon$ and ϵ being a correction that, together with the particle mobility factor, F, is sensitive to the potential parameters and HIs.

After the present Introduction, the article is organized as follows. In Sec. II we briefly explain the Brownian dynamics (BD) simulation. We also introduce the interaction potentials and the expressions of the physical quantities to be measured during the simulations. In Sec. III we present a detailed analysis and discussion of our results. Finally, the paper ends with a section of concluding remarks.

II. BROWNIAN DYNAMICS SIMULATION AND INTERACTION POTENTIALS

Diffusion in 1D channels is studied by means of BD computer simulations. We apply the same simulation methodology described in Refs. [14–16], but we now include HIs by using the Rotne-Prager mobility tensor [51]. We typically consider N particles, $N \approx 400$ with HIs and $N \approx 1000$ without HIs. Particles move in a line of length L, which is linked to the number particle density according to the expression $\rho = N/L$; L has to be chosen to guarantee the continuity of the external potential on the borders of the line; this point is discussed further below. Since particles are restricted to diffusing on the line, we only use periodic boundary conditions in the x direction in order to simulate an infinite system. The packing fraction is $\varphi = \sigma\rho$ and the mean particle distance is defined as $d \equiv \rho^{-1}$ [14–16].

The time step used in the BD simulations is $\Delta t = 2 \times 10^{-4}\,(\rho^2 D_0)^{-1}$, with $D_0 = \frac{k_B T}{6\pi\eta a}$ the free-particle diffusion coefficient of particles of radius a immersed in a solvent of viscosity η, k_B the Boltzmann constant, and T the absolute temperature. The maximum time window reached in the simulations is $t_{\max} = 500\,(\rho^2 D_0)^{-1}$, i.e., 2.5×10^6 time steps. To facilitate the analysis and reduce the set of parameters in our study, we use the following scaling factors: d for distance, d^2/D_0 for time, and $k_B T$ for energy.

A. Brownian dynamics

We now point out some details of the BD. (i) The mesoscopic size of the colloids ($\sigma \sim$ some nanometers to a few micrometers) ensures the validity of Langevin dynamics [51]. Solvent molecules are treated as variables having *fast* dynamics and they are integrated out in the dynamics of colloids, whereas the latter follow *slow* dynamics and are treated explicitly. (ii) We assume *local thermodynamic equilibrium*, i.e., particle velocities obey fast dynamics, which implies that the memory of velocities is lost much more rapidly than the time scales of interest. We are thus interested in time scales longer than the momentum relaxation time, $t \gg \tau_m = \frac{m}{6\pi\eta a}$; this is known as the diffusive temporal regime [52], with m being the mass of the colloid.

We express the discrete position Langevin equation for particle i as [52]

$$\mathbf{r}_i(t+\Delta t) = \mathbf{r}_i(t) + \left\{ \beta \sum_{j=1}^{N} \mu_{ij} \left[-\nabla_{\mathbf{r}_j} U(\mathbf{r}^{\{N\}}) + \mathbf{F}_j^{\text{ext}} \right] + \sum_{j=1}^{N} \nabla_{\mathbf{r}_j} \mu_{ij} \right\} \Delta t + \xi_i(t), \tag{4}$$

which gives us the new position of particle i at time $t + \Delta t$. Equation (4) depends on the particle position at a previous time, $\mathbf{r}_i(t)$, the net force acting on the particle and the stochastic force due to the collisions with the solvent molecules. The net force on particle i has two contributions: the force due to the particle-particle interaction and U is the total pair potential energy, and its coupling with the external field is $\mathbf{F}_i^{\text{ext}}$. HIs are also included through the Rotner-Prager mobility tensor [51,52],

$$\mu_{ii} = D_0 \mathbf{I} = \frac{k_B T}{6\pi\eta a}\mathbf{I}, \quad \mu_{ij} = \left(\frac{k_B T}{8\pi\eta r_{ij}}\right)\left(\mathbf{I} + \frac{\mathbf{r}\otimes\mathbf{r}}{r_{ij}^2}\right) + k_B T\left(a^2/4\pi\eta r_{ij}^3\right)\left(\frac{\mathbf{I}}{3} - \frac{\mathbf{r}\otimes\mathbf{r}}{r_{ij}^2}\right), \tag{5}$$

where $\mathbf{I}$ is a 3×3 unit matrix (in the 3D case) and the symbol $\otimes$ denotes a dyadic product. One notes that this mobility

tensor includes the lowest corrections of particle size over the Oseen tensor description [51] and corresponds to the case of an unbounded fluid. One thus should keep in mind that our treatment of HIs is only approximate for particles which are separated by a distance of the order of a. One notes that the mobility tensor introduces long-range interactions and couples distant particles. Equation (4) reduces to the standard Langevin equation without HIs when $\mu_{ij} \to D_0\mathbf{I}$ [14–16].

The stochastic term, $\xi(t)$, mimics the action of a thermal heat bath and obeys the fluctuation-dissipation relation [51],

$$\langle \xi_i(\Delta t)\xi_j(\Delta t)\rangle = 2\mu_{ij}\Delta t, \tag{6}$$

which is numerically implemented by a Cholesky decomposition [52,53]. We deal with the dynamics of nondeformable particles in an unbounded fluid. One can then check that $\nabla_{\mathbf{r}_j}\cdot\mu_{ij} = 0$ for the Rotner-Prager mobility tensor. This is different when we deal with a nonslip surface, where this term is nonzero and therefore should be taken into account explicitly [51,52].

B. Pair distribution function and mean-square displacement

To obtain structural information of the particle ordering along the channel, we calculate the pair distribution function, $g(x)$. The function $g(x)$ is the probability of finding a particle at a distance x from a particle located at the origin. It can be measurable in both experiments and computer simulations according to the definition [14–16]

$$g(x) = \frac{1}{N\rho}\left\langle \sum_{i=1}^{N-1}\sum_{j>i}^{N}\delta(x - x_{ij})\right\rangle, \tag{7}$$

where the angular brackets $\langle\cdots\rangle$ denote a statistical (temporal or ensemble) average.

The MSD is computed using the expression [14–16]

$$W_x(t) = \langle \Delta x(t)^2\rangle = \frac{1}{N}\sum_{i=1}^{N}\langle [x_i(t) - x_i(0)]^2\rangle. \tag{8}$$

As we see further below, at short times the MSD behaves as $W_x(t) \propto t$, i.e., normal diffusion, whereas at long times it shows a much slower power-law dependence. Then, for the sake of discussion, at long times we fit our simulation data according to the relation

$$W_x(t) = Ft^{\alpha}. \tag{9}$$

Thus, all the effects associated with the HI can be described in terms of α and the particle mobility factor F.

During our simulations, the averages are taken over at least 10 different independent stochastic realizations to reduce the statistical uncertainties. Error bars in the plots are smaller than the symbol size. For the MSD, the associated errors are statistically significant only at reduced times $tD_0/d^2 > 350$, but still, there is a clear separation between the MSD curves, and no overlap between error bars is observed during the time window used in this work.

C. Interaction potentials

We consider a system of charged colloidal particles with radius a interacting via a repulsive screened Coulomb potential. For distances $r < \sigma = 2a$, the interaction is hard-core, but for $r > \sigma$, two colloidal particles separated by a distance r interact via the repulsive part of the DLVO pair potential [14,16,54,55],

$$\beta u(r) = Z_{\text{eff}}^2\lambda_B\left[\frac{e^{\kappa a}}{1+\kappa a}\right]^2\frac{e^{-\kappa r}}{r}, \tag{10}$$

where $\beta \equiv (k_BT)^{-1}$ is the inverse of the thermal energy, Z_{eff} is the effective charge, $\lambda_B = e^2/4\pi\epsilon k_BT$ is the Bjerrum length (in international units) [56], with e the proton charge and ϵ the solvent dielectric permittivity, and κ is the Debye screening parameter [54,55]. We have used the same set of parameters as in Ref. [14]. In our study, the packing fraction, $\varphi = \sigma\rho$, is a control parameter for Yukawa systems.

Additionally, paramagnetic colloids have served as excellent models to investigate fundamental properties that are related to the role of hydrodynamics, melting transitions, order-disordered transitions, and elastic behavior in 2D crystals [44,57]. In the experiments, an external and constant magnetic field is applied in the perpendicular direction of the air-water interface [43]. This leads to a tunable quasi-long-range magnetic dipole-dipole interaction between colloids. Such an interaction can be described by the potential [44,57]

$$\beta u(r) = \frac{\Gamma}{r^3}, \tag{11}$$

where r is the reduced separation (in units of the mean particle distance) between two colloids and $\Gamma \equiv \beta(\frac{\mu_0}{4\pi})\chi_{\text{eff}}^2B^2d^{-3}$ is the mean interaction energy in units of the thermal energy, μ_0 is the vacuum susceptibility, B is the applied magnetic field, and χ_{eff} is the magnetic susceptibility of the particles. For paramagnetic colloids the potential strength, Γ, is the relevant parameter to be varied, which is equivalent to changing the particle number density because an increase in Γ results in an increase in collision rates between particles [12,44,57].

Among important experimental tools that help us to understand complex fluids are optical traps created by the interference of two laser beams [58]. In experiments, the interaction between laser beams and the colloids induces potentials with incredible precision, which permits one to create precise and strong confinement and, as a consequence, reliable control of the colloidal motion [59,60]. In recent years, optical traps have also been implemented in colloidal systems to induce an optical substrate [61], i.e., a periodic or random energy landscape. Its effect on the dynamics and the structure turned out to be fascinating [62,63].

The total external energy can then be written as $U^{\text{ext}} = \sum_{i=1}^{N}u^{\text{ext}}(\mathbf{r}_i)$, where $u^{\text{ext}}(\mathbf{r}_i)$ is the external potential, usually referred to as the substrate, acting on particle i, which here is given by the expression [14,15,63]

$$u^{\text{ext}}(\mathbf{r}_i) = V_0\sin\left(\frac{2\pi x_i}{a_L}\right), \tag{12}$$

where V_0 is the amplitude or strength of the external potential and a_L is its periodicity. Now it is appropriate to define the commensurability factor as [14,15]

$$p \equiv \frac{d}{a_L} = \frac{N}{n_{a_L}}, \tag{13}$$

where n_{a_L} is the number of sinusoidal potential periods within the channel of length L. The commensurability factor is an

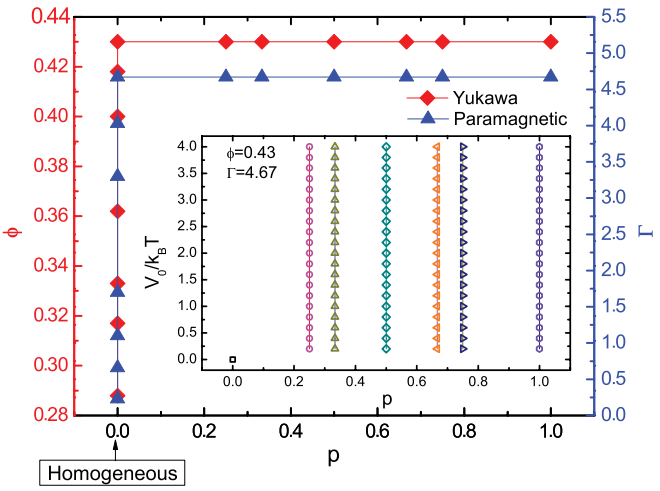

FIG. 1. (Color online) Parameter space used in the present work. The left and right vertical scales correspond to the Yukawa and paramagnetic cases, respectively. Homogeneous cases correspond to $p = 0$. Heterogeneous cases are those with $p \neq 0$. Inset: Values of the substrate strength, V_0, for each value of the commensurability factor, p.

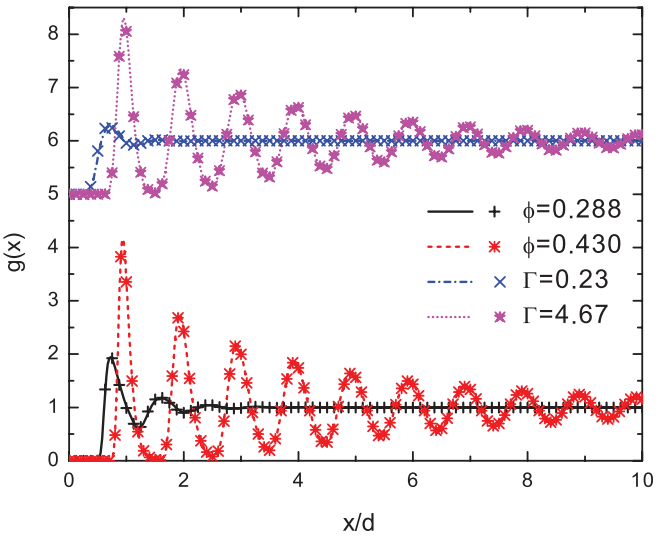

FIG. 2. (Color online) Pair distribution functions of 1D colloidal homogeneous systems. Curves are shifted for clarity. Upper curves represent superparamagnetic particles; lower curves, charged (Yukawa) colloids. Results with HIs are indicated by symbols; results without HIs, by lines.

important control parameter in our further analysis. In our simulations, L is also chosen to guarantee the continuity of the external potential on the borders of the channel.

Thus, a systematic variation of all parameters allows us to investigate the diffusive behavior of particles along the channel. We performed a detailed analysis and present only representative results here.

III. RESULTS AND DISCUSSION

Our results cover a wide range of homogeneous and heterogeneous systems, which are characterized by the set of parameters displayed in Fig. 1. The former parameters are represented by a commensurability factor $p = 0$, and the latter are explicitly described in the inset, with $\varphi = 0.43$ for charged colloids and $\Gamma = 4.67$ for superparamagnetic particles.

A. Homogeneous systems: $V_0 = 0$

It is well known that, in the absence of external fields, the static properties of any complex fluid do not depend explicitly on HIs. This simply means that in homogeneous systems, HI effects always average to 0. This provides a benchmark to test the BD methods that explicitly include HIs. We then test the reliability of our simulation method by looking at the structure of the colloids along the channel. In Fig. 2 we show the pair distribution functions, $g(x)$, of both Yukawa and superparamagnetic particles. We explicitly provide results with and without HIs and for different particle densities (low and high) and potential parameters (weak and strong couplings). We observe that $g(x)$ exhibits the typical behavior found in homogeneous fluids and recently discussed in Ref. [16]. More important is the fact that $g(x)$ does not depend on HIs. This confirms that even in 1D fluids, HIs do not affect the equilibrium structure. It also guarantees that our BD method with HIs at the level of the Rotner-Prager mobility tensor is correctly implemented.

We turn now to the MSD. We first study the case reported by Sané *et al.*, where a very short-range Weeks-Chandler-Andersen potential is used to mimic the properties of a hard-rod system [26]. Our simulation results are in good agreement with those predicted by the authors [26] (data not shown), although we do not consider the influence of walls and find that the MSD at long times is given by Eq. (1) and the mobility factor is completely described by F^{HR} [26]. Thus, we might conclude that for overdamped systems with hard-core-like interactions, the SFD is accurately determined by the theoretical approximation proposed by Kollmann [4,25].

The MSD of the systems discussed above are displayed in Fig. 3. The physical behavior of the MSD, without HIs, has also been studied in detail in Ref. [16], where it is shown that Eq. (1) describes the long-time behavior of particle diffusion along the channel and the mobility factor depends on the particle-particle interaction [see also Eq. (2)] until it reaches almost the same value at high densities (Yukawa) or strong couplings (superparamagnetic). However, we also plot those cases obtained with the explicit inclusion of HIs, which were not considered in Ref. [16]. Interestingly, we observe that for the time window indicated as "the region of interest," i.e., long times, MSDs with HIs are larger than MSDs in the absence of HIs. The reason for this behavior can be understood in terms of the long-range hydrodynamic coupling between particles (see, e.g., Refs. [43,44]). This coupling also enhances the diffusion due to *collective diffusion* induced and mediated by HIs. Collective diffusion is a dynamic process related to the cooperative movements of many particles that lead and promote collective and faster diffusion of particles in the line. We should note, interestingly, that similar collective diffusion is observed at long times in finite-size systems, i.e., circular channels, composed of particles interacting with long-range potentials and where HIs are not present [17,37].

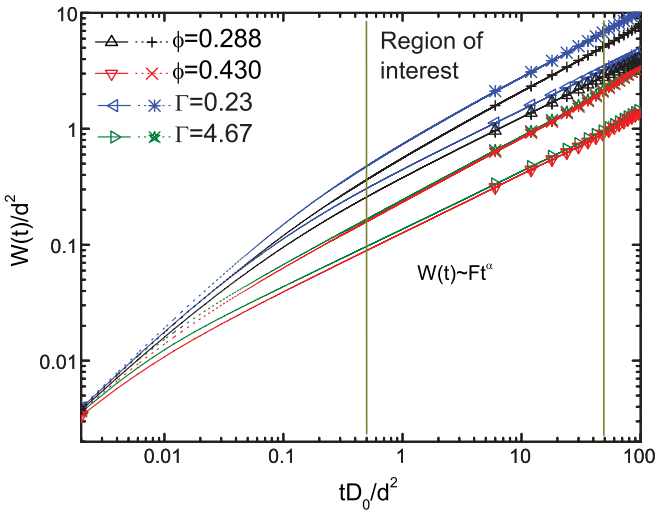

FIG. 3. (Color online) Mean-square displacements of 1D colloidal homogeneous systems: Yukawa particles and superparamagnetic colloids. Results with HIs are indicated by stars; results without HIs, by triangles. The time window where the dynamic factors, α and F, are calculated is indicated between vertical lines.

To better understand the effects of HIs on the diffusion of particles along the line, we also compute the exponent α and the mobility factor F, where the MSD can be approximated, with a high accuracy, by the power-law relation given by Eq. (9). Both parameters are depicted in Fig. 4. In general, we find that the values of the parameters predicted with the inclusion of HIs are larger than those where HIs are disregarded, but they behave in a similar way. In particular, α is 0.5 for the case without HIs, in excellent agreement with the theoretical predictions of Kollmann [25] [see Eq. (1)], and it takes the value of 0.56 with HIs and independently of the interaction

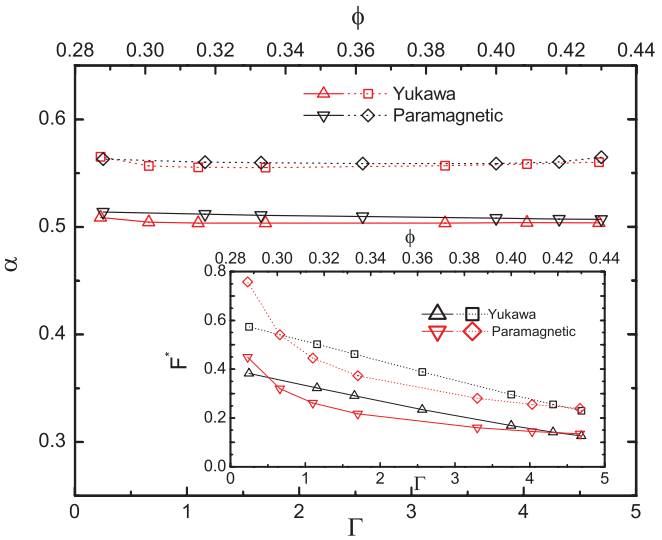

FIG. 4. (Color online) Dynamic factors, α and F, of 1D colloidal homogeneous systems as a function of the density (Yukawa particles) and coupling strengths (superparamagnetic colloids). Results with HIs are indicated by squares; results without HIs, by triangles. They were obtained by fitting the mean-square displacement to Eq. (9). Lines are guides for the eye.

potential between particles; the inclusion of HIs results in an increase of about 12% in α, which means faster, but still subdiffusive behavior. We also find that F decreases (in an exponential-like fashion) with an increase in either the density (Yukawa) or the interparticle coupling (superparamagnetic). This phenomenon is explained in Ref. [16] as follows: as the density (or potential strength) is increased, the colloids are more localized and just oscillate around their equilibrium positions; at this point, the highly packed fluid consists of a quasi–regularly spaced sequence of particles where the relative distance is represented to within a few percent by $1/\rho$.

B. Heterogeneous systems: $V_0 \neq 0$

One-dimensional colloidal systems under periodic energy landscapes show interesting structural and dynamic properties. For example, it is observed that the competition between both particle-particle and particle-field interactions gives rise to a rich variety of adsorbate phases [14]. It has also been demonstrated that the action of the external field leads to very interesting phenomena, such as the localization of particles and, under special conditions, to depinning-like effects, which are observed in an enhancement of the mobility factor and a loss of spatial correlation along the line [14,15]. Thus, the study of particle diffusion in energy landscapes turns out to be fascinating and, even more, complex when HIs are taken into account explicitly.

Before we discuss our results in detail, we should point out that in previous work two of us studied the MSD for $p \gtrsim 1$ and found that its long-time behavior follows the power law given by Eq. (1). Hence, in the present section we explore the influence of the external sinusoidal potential [see Eq. (12)] in an extended regime of commensurabilities, i.e., $0 < p \leqslant 1$, and its consequences on the dynamical properties of particles moving in periodic energy landscapes. The potential parameters are displayed in Fig. 1.

1. Yukawa particles

For the sake of discussion and for illustrative purposes, we show in Fig. 5 the equilibrium positions of Yukawa particles along the line. The energy landscape imposed by the external field is depicted by sinusoidal curves, which are shifted in the vertical direction for clarity. One can note that the variation of the number of particles per potential minima is dictated by the commensurability factor p. Regarding the structure, we do not observe considerable differences when HIs are explicitly included (data not shown). Thus, from here on, we focus our attention on the dynamical properties.

We start by analyzing the behavior of α, which is displayed in Fig. 6. Figure 6(a) shows cases with $p \leqslant 1/2$, and Fig. 6(b), with $1/2 < p \leqslant 1$. In the former cases, we observe that, except for $p = 1/2$, $\alpha = 0.5$ and $\alpha \approx 0.6$ without and with HIs, respectively. This behavior is independent of the coupling parameter V_0. This means that the particles experience faster diffusion due to their hydrodynamical coupling with the external potential. However, for $p = 1/2$, particles will diffuse more slowly for $V_0 \gtrsim 1.8 k_B T$, even without considering HIs explicitly; this slow decay should be associated with the distribution of particles along the sinusoidal field. This point is discussed in more detail below.

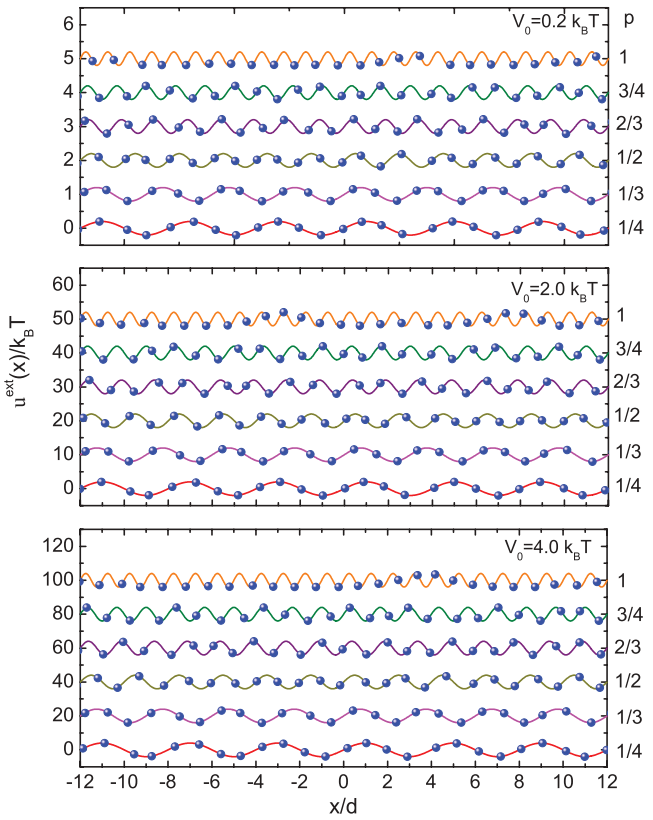

FIG. 5. (Color online) Circles: Equilibrium positions of Yukawa particles along the line for different values of the commensurability factor p (1/4, 1/3, 1/2, 2/3, 3/4, 1). Three values of the external coupling strength, V_0, are displayed. Solid lines: Sinusoidal contribution of the external potential [see Eq. (12)]. Curves are shifted in the vertical direction for clarity. The packing fraction is $\varphi = 0.43$ and the parameters of the external field are indicated in the inset in Fig. 1.

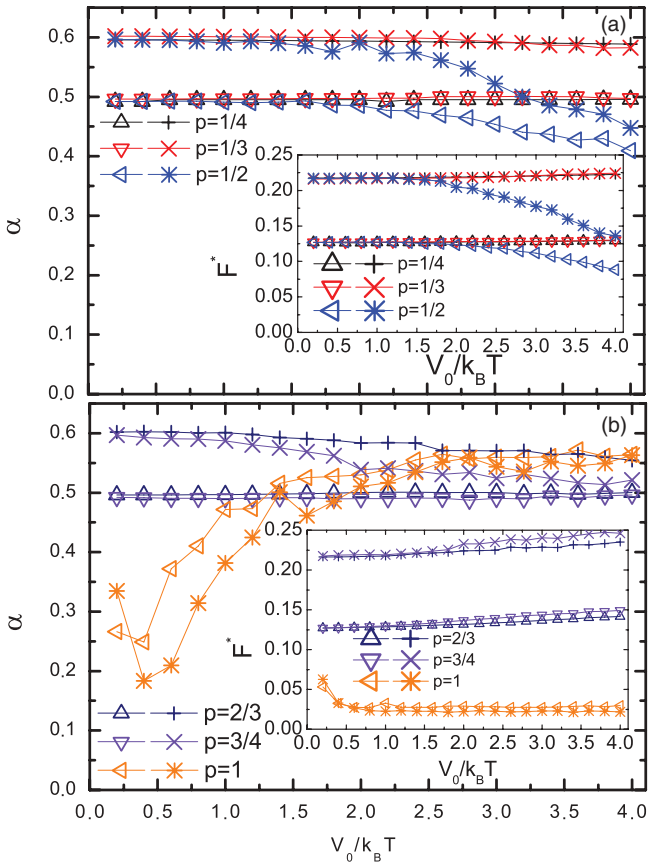

FIG. 6. (Color online) Dynamic factors, α and F, that characterize the diffusion of Yukawa particles as a function of the coupling strength, V_0, for different commensurability scenarios. The packing fraction is $\phi = 0.43$. We show results with (stars) and without (open triangles) HIs. Lines are guides for the eye.

For $p > 1/2$ [see Fig. 6(b)] the following interesting features are noted: (i) for $p = 2/3$ and $p = 3/4$, diffusive behavior occurs with the characteristic exponent $\alpha = 0.5$, i.e., normal SFD, when HIs are neglected; however, with the inclusion of HIs the diffusive behavior is $\alpha \approx 0.6$, but it decreases with V_0, reaching a saturation value of $\alpha \approx 0.55$ for $p = 2/3$ and $\alpha \approx 0.5$ for $p = 3/4$. The latter is in good agreement with Ref. [14], where the commensurability factor $p \approx 0.82$ was investigated. (ii) $p = 1$ exhibits nonmonotonic behavior, with a minimum located at $V_0 \approx 0.4 k_B T$. After this point, the diffusion becomes faster, until it reaches a plateau of about $\alpha \approx 0.55$. However, contrary to the previous cases, the inclusion of HIs led to a completely unexpected slower diffusion when $V_0 \gtrsim 0.6 k_B T$. This behavior is explained below.

So far we have found that, except for $p = 1$, HIs promote faster particle diffusion compared with the case without HIs, but the exponent α depends on the coupling with the external potential. Thus, to understand the dynamical scenario discussed above, we now use simple physical arguments to better appreciate the competition between the particle-particle potential and the accommodation of the particles on the potential minima along the line. The way in which particles are accommodated in the channel depends on the particular choice of p. For example, the difference between $p = 1/4$ and $p = 3/4$ resides in the fact that for the former there are four particles per potential minimum, and for the latter, four particles are distributed over three potential minima. This can best be seen in Fig. 5.

Then, for $p = 1/2$ both F and α show decay starting at about $V_0/k_B T = 2.0$. This case corresponds to two particles per minimum. Thus, from an energetic point of view, the pair of particles is competing for their localization at the minimum (see Fig. 5 for $p = 1/2$), but due to their repulsive interaction [see Eq. (10)], they will never be in contact, and as a consequence, they cannot be located at the minimum. However, the pair behaves like an effective *dimer* whose center of mass is, on average, at the position of the potential minimum. When V_0 is small ($<2k_B T$), due to thermal fluctuations, the dimers overcome the well depth and also the energetic barrier induced by the surrounding dimers, i.e., weak localization. Thus, normal SFD is found without including HIs and $\alpha = 0.6$ with HIs. For larger V_0 ($>2k_B T$), the dimers turn out to be more strongly localized around the minimum, with each particle of the effective dimer trying to occupy the potential minimum. This competition makes collective diffusion harder and diffusion of the entire line becomes slower even in the presence of hydrodynamical coupling.

In contrast to $p = 1/2$, the dynamical behavior for the case $p = 1$ is more complex and less intuitive. First, this case corresponds to one particle per minimum (see Fig. 5 for $p = 1$). Our results reveal three dynamical regimes: (i) very weak coupling ($V_0 < 0.6k_BT$), which shows a decrease in diffusion; (ii) weak coupling ($0.6k_BT \lesssim V_0 \lesssim 1.6k_BT$), which exhibits an increase in diffusion; and (iii) strong coupling ($V_0 > 1.6k_BT$), where an almost-normal SFD is observed. The latter regime is consistent with the results presented in Ref. [14]. In all the regimes, diffusion is subdiffusive, i.e., $\alpha < 1$. However, it is important to stress that for very weak couplings, as expected, HIs describe faster diffusion than in the situation without HIs; in the limit $V_0 \ll k_BT$, the value 0.6 is recovered (data not shown). Nonetheless, at weak and strong couplings the opposite scenario is found: hydrodynamical coupling among particles leads to slower diffusion. This behavior is completely unexpected, since for the other commensurability factors HIs promoted faster diffusion. Thus, in these regimes HIs give rise to *anticooperative* dynamics, which can be associated with a possible increase in energy dissipation due to friction with the solvent. Moreover, for $p = 1$ every colloid could be, on average, located at the potential minimum. When this condition is satisfied, a collective dynamics along the line emerges and the diffusion is given by the normal SFD; this scenario is observed at strong couplings, where the external field forces the particles to occupy the potential minima. This is the same mechanism that allows us to observe the exponential decay of the correspondingly reduced mobility factor displayed in the inset in Fig. 6 [16]. Unfortunately, the complexity of the dynamics at weak couplings cannot be entirely explained in terms of the competition to occupy the potential minimum of the external field.

To visualize in a better way the nonmonotonic dependence of the particle dynamics for $p = 1$, we show in Fig. 7 the MSD for different values of V_0, which are chosen according to the dynamical regimes discussed above. At short times,

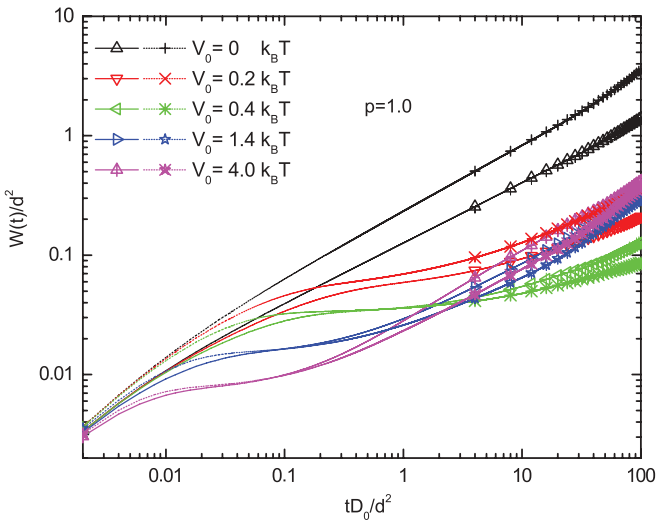

FIG. 7. (Color online) Mean-square displacements of 1D Yukawa particles on a sinusoidal potential given by Eq. (12) with a commensurability factor $p = 1$ and different values of the external potential strength V_0. Results with HIs are indicated by stars; results without HIs, by triangles.

diffusion is normal and independent of both the interparticle interaction and the external potential. At intermediate times the dynamics becomes subdiffusive (in all cases), with an almost-well-defined plateau, which indicates that the particle spends a considerable time on the potential minimum. However, the long-time behavior shows an unexpected nonmonotonic variation that strongly depends on the external potential strength V_0. This is the evidence of the nontrivial and complex competition between particle-particle and particle-substrate interactions that leads to the dynamical factors displayed in Fig. 6.

The behavior of the reduced mobility factor, F^*, is also depicted in Fig. 6. The mobilities calculated with inclusion of HIs for $p \neq 1$ are higher than those obtained without them, as in the homogeneous case. Thus, HIs allow faster motion and strong dynamic couplings, which lead to collective motions that result in an enhancement of particle mobility. For $p = 1/4$, $1/3$, $2/3$, and $3/4$ (see Fig. 5), F shows a slow increase with V_0, being more noticeable for $p = 3/4$. The latter effect has been investigated in Ref. [14]. The increase in the mobility factor, even larger than in the homogeneous case (see inset in Fig. 4), is due to the noise-assisted effect, in which thermal fluctuations act cooperatively, leading to a higher particle mobility [14]. The enhancement of F also reveals a depinning of the line from its sinusoidal substrate. Thus, HIs contribute to this noise-assisted effect due to the fact that they promote the diffusion of particles and provide the opportunity for particles to be less pinned to the external field.

2. *Paramagnetic colloids*

In order to answer the question whether the previous dynamical scenario depends on the kind of interaction potential, we turn now to the case of superparamagnetic colloids, where particles interact with a long-range potential given by Eq. (11). In the following paragraphs we focus on the similarities and differences among the dynamical properties exhibited by both superparamagnetic and Yukawa particles. We should mention that in previous Yukawa many-particle systems, the screening parameter κ was chosen in the intermediate range such that nearest-neighbor particles are correlated but the interparticle interaction is completely screened for larger distances.

Due to the strong repulsion, paramagnetic colloids show particle configurations along the line similar to those of Yukawa particles (see Fig. 8). In this case, we consider that the long-time behavior of the MSD scales as $\propto t^{\alpha}$ and can be fitted according to Eq. (9). The external potential parameters are depicted in Fig. 1 and the corresponding dynamic factors, α and F, are displayed in Fig. 9.

For $p < 1/2$ we find that α is independent of the nature of the repulsive interaction potential among the particles and the inclusion of Hls promotes faster diffusion. For $1/2 < p < 1$ we observe that α decays slowly when $V_0 \gtrsim 1.0k_BT$; it decreases, reaching a saturation value of $\alpha \approx 0.54$ for $p = 2/3$ and $\alpha \approx 0.52$ for $p = 3/4$. The latter is in good agreement with Ref. [15] for $p \approx 0.82$. In the particular case where $p = 1/2$, it decays at smaller values of V_0 and its magnitude is also smaller than that obtained for Yukawa particles. This means that the dynamics of superparamagnetic particles is slightly slower. This can also be associated with the accommodation

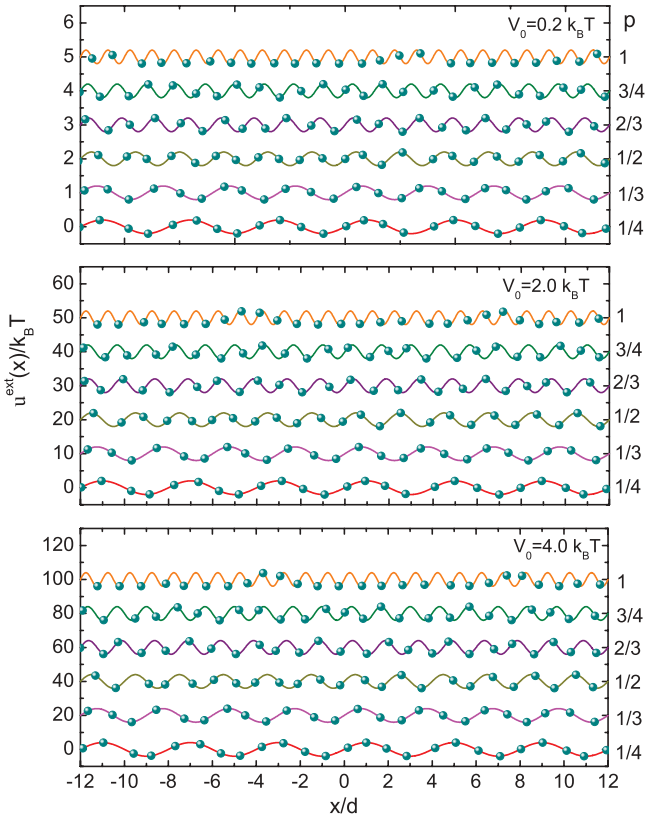

FIG. 8. (Color online) Circles: Equilibrium positions of superparamagnetic colloids along the line for different values of the commensurability factor p (1/4, 1/3, 1/2, 2/3, 3/4, 1). Three values of the external coupling strength, V_0, are displayed. Solid lines: Sinusoidal contribution of the external potential [see Eq. (12)]. Curves are shifted in the vertical direction for clarity. The coupling parameter $\Gamma = 4.67$ and the parameters of the external field are indicated in the inset in Fig. 1.

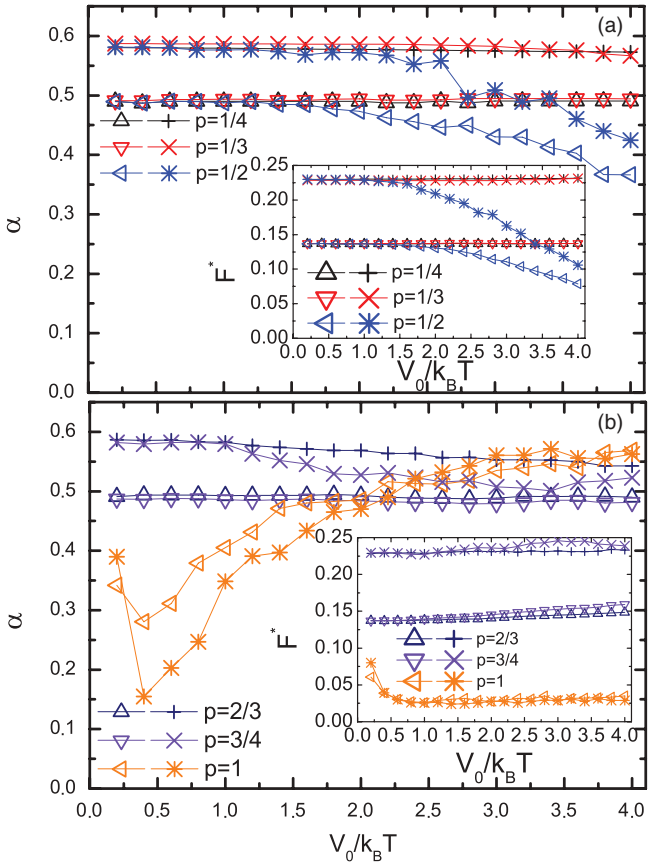

FIG. 9. (Color online) Dynamic factors, α and F, that characterize the diffusion of superparamagnetic colloids as a function of the coupling strength, V_0, for different commensurability scenarios. The coupling parameter $\Gamma = 4.67$. We show results with (stars) and without (open triangles) HIs. Lines are guides for the eye.

of the particles on the potential minima. From Fig. 8, we still see effective dimers around some minima, however, we can also appreciate that some particles are located on the maxima (in this case the probability is higher) due to the stronger repulsion at short distances and the long-range spatial correlation between particles. This increases the contribution of the interparticle potential to the particle distribution along the sinusoidal substrate. In fact, we can argue that particles find meta-stable equilibrium positions that are not frequently observed when the interaction potential is short-range and, consequently, makes collective diffusion in the channel more difficult.

For $p = 1$ we have similar dynamical regimes: (i) very weak coupling ($V_0 < 0.4k_BT$), which shows a decrease in diffusion; (ii) weak coupling ($0.4k_BT \lesssim V_0 \lesssim 2.0k_BT$), which exhibits an increase in diffusion; and (iii) strong coupling ($V_0 > 2.0k_BT$). The transition from weak to strong coupling is located at larger V_0 ($>2k_BT$) than for Yukawa particles. Interestingly, this strong-coupling dynamical region seems to be, in both cases, almost independent of HIs and the kind of interaction between particles ($\alpha \approx 0.55$).

The insets in Fig. 9 show the behavior of F for different values of p and V_0. Specifically, for $p < 1/2$ and $1/2 < p < 1$ there is an increase in the mobility factor, which is more dramatic for $V_0/k_BT \geqslant 2.0$ and similar to that for Yukawa particles. For $p = 1/2$, the decrease in the mobility factor for $V_0/k_BT \geqslant 2.0$ is larger than the decay of F shown by Yukawa particles [see inset in Fig. 9(a)]. Thus, superparamagnetic colloids exhibit stronger *noncooperative* behavior than Yukawa particles. Moreover, as in the case of Yukawa particles, for $p = 1$ we find that F decays exponentially [see inset in Fig. 9(b)]. This confirms that the behavior of F imposed by the external field is present regardless of the kind of repulsive interaction potential between particles [16].

IV. CONCLUDING REMARKS

We have theoretically investigated the effects due to HIs on the diffusive properties of repulsively interacting colloids confined in a 1D channel and subjected to a periodic external potential. We have considered two types of interparticle interactions, namely, Yukawa and super-paramagnetic potentials. We have performed an extensive study covering an extended parameter space that includes weak and strong couplings among particles and different values of the external potential strength. We found that, in general, the complex dynamical scenarios of both systems are basically the same because both potentials lead to a correlation of the

particles at long interparticle separations. A different behavior is thus expected with attractive and repulsive short-range potentials.

We also found that HIs lead to an enhancement of the particle mobility. In particular, the MSD exhibits subdiffusive behavior at long times and it scales as a power law $W(t) \propto t^{\alpha}$, with $\alpha < 1$. In homogeneous systems, we found that α deviates from the normal SFD and takes the value of $\alpha \approx 0.6$. When the external potential is switched on, particle diffusion became sensitive to the strength and commensurability of the sinusoidal potential with the interparticle spacing. Most of the dynamical properties can be explained in terms of collective diffusion, due to the long-range nature of the HIs, and the competition between particle-particle and particle-substrate interactions. The latter are responsible for the particle accommodation on the minima of the external potential. However, the case $p = 1$ is particular due to the fact that the system exhibits three dynamical regimes, which still need to be explored in detail in order to understand the dynamical anticooperative behavior imposed, in this case, by HIs.

Last, but not least, we must point out that our simulations have allowed us to extend the understanding of the SFD in systems composed of interacting Brownian particles under 1D modulated energy landscapes and the action of HIs. These results could be corroborated in experiments with light force fields.

ACKNOWLEDGMENTS

This work was partially supported by the "Odysseus" Program of the Flemish Government, the Flemish Science Foundation (FWO-Vl), and PIFI 3.4—PROMEP and CONACyT (Grant Nos. 61418/2007 and 102339/2008, Ph.D. Scholarship No. 230171/2010).

[1] G. Nägele, Phys. Rep. **272**, 215 (1996).
[2] C. Lutz, M. Kollmann, and C. Bechinger, Phys. Rev. Lett. **93**, 026001 (2004).
[3] C. Lutz, M. Kollmann, P. Leiderer, and C. Bechinger, J. Phys.: Condens. Matter **16**, S4075 (2004).
[4] B. Lin, M. Meron, B. Cui, S. A. Rice, and H. Diamant, Phys. Rev. Lett. **94**, 216001 (2005).
[5] B. Lin, B. Cui, J.-H. Lee, and J. Yu, Europhys. Lett. **57**, 724 (2002).
[6] X. Xu, B. Lin, B. Cui, A. R. Dinner, and S. A. Rice, J. Chem. Phys. **132**, 084902 (2010).
[7] D. T. Valley, S. A. Rice, B. Cui, H. M. Ho, H. Diamant, and B. Lin, J. Chem. Phys. **126**, 134908 (2007).
[8] X. Xu and S. A. Rice, J. Chem. Phys. **122**, 024907 (2005); http://link.aip.org/link/?JCP/122/024907/1.
[9] X. Xu, S. A. Rice, B. Lin, and H. Diamant, Phys. Rev. Lett. **95**, 158301 (2005).
[10] A. Taloni and F. Marchesoni, Phys. Rev. Lett. **96**, 020601 (2006).
[11] B. Cui, B. Lin, S. Sharma, and S. A. Rice, J. Chem. Phys. **116**, 3119 (2002).
[12] Q.-H. Wei, C. Bechinger, and P. Leiderer, Science **287**, 625 (2000).
[13] K. Nelissen, V. R. Misko, and F. M. Peeters, Europhys. Lett. **80**, 56004 (2007).
[14] S. Herrera-Velarde and R. Castañeda-Priego, J. Phys.: Condens. Matter **19**, 226215 (2007).
[15] S. Herrera-Velarde and R. Castañeda-Priego, Phys. Rev. E **77**, 041407 (2008).
[16] S. Herrera-Velarde, A. Zamudio-Ojeda, and R. Castaneda-Priego, J. Chem. Phys. **133**, 114902 (2010).
[17] D. V. Tkachenko, V. R. Misko, and F. M. Peeters, Phys. Rev. E **80**, 051401 (2009).
[18] P. Hänggi and F. Marchesoni, Rev. Mod. Phys. **81**, 387 (2009).
[19] T. Harris, *Diffusion with "Collisions" Between Particles*, Memorandum (Rand Corporation, Santa Monica, CA, 1965); http://books.google.be/books?id=BXm3PAAACAAJ.
[20] R. Arratia, Ann. Probabil. **11**, 362 (1983).
[21] D. G. Levitt, Phys. Rev. A **8**, 3050 (1973).
[22] J. K. Percus, Phys. Rev. A **9**, 557 (1974).
[23] J. Kärger, Phys. Rev. A **45**, 4173 (1992).
[24] K. Hahn, J. Kärger, and V. Kukla, Phys. Rev. Lett. **76**, 2762 (1996).
[25] M. Kollmann, Phys. Rev. Lett. **90**, 180602 (2003).
[26] J. Sane, J. T. Padding, and A. A. Louis, Faraday Discuss. **144**, 285 (2010).
[27] G. Coupier, M. Saint Jean, and C. Guthmann, Phys. Rev. E **73**, 031112 (2006).
[28] J. B. Delfau, C. Coste, C. Even, and M. Saint Jean, Phys. Rev. E **82**, 031201 (2010).
[29] J. B. Delfau, C. Coste, and M. Saint Jean, Phys. Rev. E **85**, 041137 (2012).
[30] J. B. Delfau, C. Coste, and M. Saint Jean, Phys. Rev. E **85**, 061111 (2012).
[31] C. Coste, J.-B. Delfau, C. Even, and M. Saint Jean, Phys. Rev. E **81**, 051201 (2010).
[32] G. Piacente, I. V. Schweigert, J. J. Betouras, and F. M. Peeters, Phys. Rev. B **69**, 045324 (2004).
[33] L. Lizana and T. Ambjörnsson, Phys. Rev. Lett. **100**, 200601 (2008).
[34] T. Ambjörnsson, L. Lizana, M. A. Lomholt, and R. J. Silbey, J. Chem. Phys. **129**, 185106 (2008).
[35] T. Ambjörnsson and R. J. Silbey, J. Chem. Phys. **129**, 165103 (2008).
[36] L. Lizana and T. Ambjörnsson, Phys. Rev. E **80**, 051103 (2009).
[37] D. Lucena, D. V. Tkachenko, K. Nelissen, V. R. Misko, W. P. Ferreira, G. A. Farias, and F. M. Peeters, Phys. Rev. E **85**, 031147 (2012).
[38] D. V. Tkachenko, V. R. Misko, and F. M. Peeters, Phys. Rev. E **82**, 051102 (2010).
[39] S. Varga, G. Ballo, and P. Gurin, J. Stat. Mech. (2011) P11006.
[40] S. J. Manzi, J. J. Torrez Herrera, and V. D. Pereyra, Phys. Rev. E **86**, 021129 (2012).

[41] Q.-H. Wei, C. Bechinger, and P. Leiderer, in *Trends in Colloid and Interface Science XIII, Progress in Colloid and Polymer Science*, Vol. 112, edited by D. Težak and M. Martinis (Springer, Berlin, 1999), pp. 227–230.
[42] T. R. Stratton, S. Novikov, R. Qato, S. Villarreal, B. Cui, S. A. Rice, and B. Lin, Phys. Rev. E **79**, 031406 (2009).
[43] K. Zahn, J. M. Méndez-Alcaraz, and G. Maret, Phys. Rev. Lett. **79**, 175 (1997).
[44] B. Rinn, K. Zahn, P. Maass, and G. Maret, Europhys. Lett. **46**, 537 (1999).
[45] T. Franosch, M. Grimm, M. Belushkin, F. M. Mor, G. Foffi, L. Forron, and S. Jeney, Nature (London) **478**, 85 (2011).
[46] J. C. Meiners and S. R. Quake, Phys. Rev. Lett. **82**, 2211 (1999).
[47] M. Reichert and H. Stark, Phys. Rev. E **69**, 031407 (2004).
[48] R. Fitzgerald, Phys. Today **54**, 18 (2001).
[49] A. Ryabov and P. Chvosta, Phys. Rev. E **83**, 020106(R) (2011).
[50] R. D. L. Hanes, C. Dalle-Ferrier, M. Schmiedeberg, M. C. Jenkins, and S. U. Egelhaaf, Soft Matter **8**, 2714 (2012).
[51] J. K. G. Dhont, *An Introduction to Dynamics of Colloids* (Elsevier, Amsterdam, 1996).
[52] M. Manghi, X. Schlagberger, Y.-W. Kim, and R. R. Netz, Soft Matter **2**, 653 (2006).
[53] M. P. Allen and D. J. Tildesley, *Computer Simulation of Liquids* (Clarendon Press, New York, 1989).
[54] P. Debye and E. Hückel, Phys. Z. **24**, 185 (1923); http://electrochem.cwru.edu/estir/hist/hist-12-Debye-1.pdf.
[55] E. J. W. Verwey and Overbeek, *Theory of the Stability of Lyophobic Colloids* (Elsevier, Amsterdam, 1948).
[56] L. F. Rojas-Ochoa, R. Castañeda-Priego, V. Lobaskin, A. Stradner, F. Scheffold, and P. Schurtenberger, Phys. Rev. Lett. **100**, 178304 (2008).
[57] S. Herrera-Velarde and H. H. von Grunberg, Soft Matter **5**, 391 (2009).
[58] A. Ashkin, Proc. Natl. Acad. Sci. USA **94**, 4853 (1997).
[59] E. M. Furst, Curr. Opin. Coll. Surf. Sci. **10**, 79 (2005).
[60] M. C. Jenkins and S. U. Egelhaaf, J. Phys.: Condens. Matter **20**, 404220 (2008).
[61] C. Bechinger and E. Frey, *Soft Matter*, edited by G. Gompper and M. Schick (Wiley-VCH, New York, 2007), Vol. 3, p. 87.
[62] K. Dholakia and T. Čižmár, Nat. Photon. **5**, 335 (2011).
[63] S. Herrera-Velarde and R. Castañeda-Priego, Phys. Rev. E **79**, 041407 (2009).